Gradient, High Resolution, Magic Angle Sample Spinning NMR

W. E. Maas,[†] F. H. Laukien,[†] and D. G. Cory*,[‡]

Bruker Analytical Systems, Inc.
15 Fortune Drive, Billerica, Massachusetts 01821
Department of Nuclear Engineering, NW14-4111
150 Albany Street, Massachusetts Institute of Technology
Cambridge, Massachusetts 02139

Received July 1, 1996

Recently a number of NMR studies have been reported in which magic angle sample spinning (MAS) was applied to increase the resolution of spectra from non-solid materials. Examples include polymer gels,[1] lipids,[2] tissue samples,[3] and swollen resins[4−6] used as supports in combinatorial chemistry. While these samples generally have sufficient mobility to greatly average anisotropic interactions, the spectral resolution for the static samples is still much lower than that which is achieved for liquid samples. The excess broadening under static conditions is due to a combination of residual dipolar interactions and variations in the bulk magnetic susceptibility.[7] The above studies convincingly demonstrate that MAS is efficient at averaging these left-over components of the solid state line width, and lead to NMR spectra that display resolution approaching that of liquid samples. Such methods have been termed high-resolution MAS (hr-MAS) NMR.

Hr-MAS NMR is of particular importance in the area of combinatorial chemistry, where it is promoted as a means of obtaining high-resolution NMR spectra of material bound to the support, and thereby without disrupting a complex synthesis. This capability is viewed as central to the continued successful implementation of combinatorial chemistry methods.[4,6]

Here we report on a further development of hr-MAS measurements that leads to significant advances in this type of spectroscopy, the addition of a magnetic field gradient (g-hr-MAS). As in high resolution liquid state studies, the gradient is essential for removing t_1 noise and is extremely helpful in coherence pathway selection. As will be discussed, in the simplest implementation, the spatially varying field strength seen by a spin packet over time should not vary, and therefore, since the sample is moving, the gradient is best applied in a reference frame that is tied to this motion.

Based on the broad acceptance of gradient methods in high resolution solution state NMR studies, it is not surprising that gradients can be of use in hr-MAS measurements, particularly since the NMR methods are adopted from the liquid state (rather than the solid state) class of methods. What may not be appreciated is the extra role gradients play in the presence of MAS. The sample spinning introduces two additional modulations into the experiment. Even though the most common RF coil configuration is a solenoid, the finite wire size and discrete wire placement lead to significant RF field inhomogeneities and therefore to signal modulations in the presence of sample rotation. The RF inhomogeneity results in a coherent modulation of the RF intensity as the sample is spun (assuming a uniformly packed rotor), which is clearly observed as extra sidebands in MAS homonuclear correlation experiments. The spinner dynamics also introduce an overall modulation of the sample coupling to the receiver (Q-modulation) which appears as an incoherent modulation, since the pulse experiment is not normally synchronized to the spinning frequency. The incoherent term results in a broad spectrum of t_1 noise and is the effect seen most easily in heteronuclear measurements. Magnetic field gradients may be employed to suppress both of these artifacts, by dephasing magnetization components that do not follow a prescribed coherence pathway, prior to acquisition.

For certain solid state imaging experiments, gradient coils have been added to MAS probes, the focus being to create an imaging reference frame tied to the spinning sample rather than the conventional stationary laboratory reference frame. Such means were suggested by Wind and Yannoni,[8] implemented by Cory and Veeman[9] and others.[10,11] In all of these approaches the gradient fields were made to rotate with the sample by modulating the currents (through specially designed gradient coils) synchronously with the spinning. For high resolution liquid state experiments, Bowtell[12] has described a gradient set that creates a gradient field oriented along the magic angle through a current distribution confined to a cylinder oriented along the static field. This arrangement was proposed to avoid interference from dipolar demagnetizing fields[13] and is not compatible with conventional MAS probe designs.

In order to implement gradient spectroscopy experiments in a MAS probe the gradient should introduce a resonance that is not temporally modulated. This may be accomplished with a time-independent gradient field where the gradient is oriented such that the *z* component of the magnetic field increases along the axis of the spinner and the *z* component of the magnetic field gradient is uniform in the planes perpendicular to the spinner axis.

The role of the gradient—and the necessary geometry—is most easily seen by exploring the time variation of the *z* component of the magnetic field gradient under magic angle sample spinning. A coordinate system that is tied to the rotating sample is described by two Unitary transformations from the stationary laboratory reference frame, a tilt of the laboratory frame (x, y, z) to a magic angle frame (x_m, y_m, z_m), followed by a rotation to the MAS frame (x_s, y_s, z_s).

$$\begin{pmatrix} x_s \\ y_s \\ z_s \end{pmatrix} = \begin{pmatrix} \cos(\omega_s t) & \sin(\omega_s t) & 0 \\ -\sin(\omega_s t) & \cos(\omega_s t) & 0 \\ 0 & 0 & 1 \end{pmatrix} \begin{pmatrix} 1 & 0 & 0 \\ 0 & \cos\theta_m & -\sin\theta_m \\ 0 & \sin\theta_m & \cos\theta_m \end{pmatrix} \begin{pmatrix} x \\ y \\ z \end{pmatrix}$$

A straightforward and general approach to designing gradient coils is to first specify the Jacobian that describes the variation of the magnetic field and then to translate this into a current distribution. The Jacobian has the form,

$$J = \begin{pmatrix} \partial B_x/\partial x & \partial B_x/\partial y & \partial B_x/\partial z \\ \partial B_y/\partial_x & \partial B_y/\partial y & \partial B_y/\partial z \\ \partial B_z/\partial x & \partial B_z/\partial y & \partial B_z/\partial z \end{pmatrix}$$

In NMR experiments the spin system is only sensitive to static fields along the same direction as the externally applied magnetic field, therefore the experiment geometry only uniquely

---

* Author to whom correspondence should be addressed.

[†] Bruker Analytical Systems, Inc.

[‡] Massachusetts Institute of Technology.

(1) Styver, H. D. H.; Fræchet, J. M. J. *Macromolecules* **1991,** *24*, 883.

(2) Gross, J. D.; Costa, P. R.; Dubacq, J. B.; Warschawski, D. E.; Lirsca, P. N.; Devaux, P. F.; Griffin, R. G. *J. Magn. Reson*. **1995**, *106*, 187.

(3) Cheng, L. L.; Lean, C. L.; Bogdanova, A.; Wright S. C., Jr.; Ackerman, J. L.; Brady, T. J.; Garrido, L. *Magn. Reson. Med*. In press.

(4) Anderson, R. C.; Jarema, M. A.; Shapiro, M. J.; Stokes, J. P. Ziliox, M. *J. Org. Chem*. **1995**, *60*, 2650.

(5) Keifer, P.; Baltusis, L.; Rice, D. M.; Tymiak, A.; Shoolery, J. N. *J. Magn. Reson*. **1996**, *A119*, 65.

(6) Sarkar, S. K.; Garigipati, R. S.; Adams, J. L.; Keifer, P. A. *J. Am. Chem. Soc*. **1996**, *118*, 2305.

(7) Garroway, A. N. *J. Magn. Reson*. **1982**, *49*, 168.

(8) Wind, R.; Yannoni, C. S. U.S. Patent 4 301 410, 17 November 1981.

(9) Cory, D. G.; van Os, J. W. M.; Veeman, W. S. *J. Magn. Reson*. **1989**, *76*, 543.

(10) Schau¢, G.; BlÚmich, B.; Spiess, H. W. *J. Magn.Reson*. **1991**, *95*, 437.

(11) Buszko, M.; Maciel, G. E. *J. Magn.Reson*. **1994,** *A107*, 151.

(12) Bowtell, R.; Peters, A. *J. Magn. Reson*. **1995**, *A115*, 55.

(13) Warren, W. S.; Richter, W.; Hamilton Andreotti, A.; Farmer, B. T., II *Science*, **1993**, *262*, 2005.

S0002-7863(96)02227-5 CCC: $12.00

specifies the three components,

$$\partial B_z/\partial x,\ \partial B_z/\partial y,\ \partial B_z/\partial z$$

The time dependence of the field seen by a spinning sample is therefore contained in the transformation of this vector to the MAS frame,

$$B(r_s,t) = \begin{pmatrix} \cos(\omega_s t) & \cos\theta_m \sin(\omega_s t) & -\sin\theta_m \sin(\omega_s t) \\ -\sin(\omega_s t) & \cos\theta_m \cos(\omega_s t) & -\sin\theta_m \cos(\omega_s t) \\ 0 & \sin\theta_m & \cos\theta_m \end{pmatrix} \begin{pmatrix} \partial B_z/\partial x \\ \partial B_z/\partial y \\ \partial B_z/\partial z \end{pmatrix} \cdot \begin{pmatrix} x \\ y \\ z \end{pmatrix}$$

with a desired solution—in this magic angle frame—of the form,

$$B(r_s,t) = \begin{pmatrix} 0 \\ 0 \\ \partial B_z/\partial \theta_m \end{pmatrix}$$

leading to the three simultaneous equations,

$$\cos(\omega_s t)\frac{\partial B_z}{\partial x} + \cos\theta_m \sin(\omega_s t)\frac{\partial Bz}{\partial y} - \sin\theta_m \sin(\omega_s t)\frac{\partial B_z}{\partial z} = 0$$

$$-\sin(\omega_s t)\frac{\partial B_z}{\partial x} + \cos\theta_m \cos(\omega_s t)\frac{\partial B_z}{\partial y} - \sin\theta_m \cos(\omega_s t)\frac{\partial B_z}{\partial z} = 0$$

$$\sin\theta_m \frac{\partial B_z}{\partial y} + \cos\theta_m \frac{\partial B_z}{\partial z} = \frac{\partial B_z}{\partial \theta_m}$$

The only solution for this geometry of gradient field that is consistent with a time independent magnetic field gradient along the z_s axis is,

$$\frac{\partial B_z}{\partial x} = 0,\ \frac{\partial B_z}{\partial y} = \sin\theta_m \frac{\partial B_z}{\partial \theta_m},\ \frac{\partial B_z}{\partial z} = \cos\theta_m \frac{\partial B_z}{\partial \theta_m}$$

These conditions do not completely define the Jacobian, there are a manifold of solutions to Maxwell's equations that are consistent with the values of these three components. For the work reported here, we chose a proprietary coil geometry where $\partial B_x/\partial x, y, z = 0$, and which is compatible with commonly used MAS stator designs.[14]

A series of heteronuclear correlation experiments (HMQC and HMBC) are shown in Figures 1 and 2 to demonstrate the level of artifact suppression available with gradients in hr-MAS spectra. The sample, an N-FMOC-N-Boc-L-Lysine derivatized Wang resin swollen with $CDCl_3$, was placed in a 4 mm o.d. zirconia rotor and spun at 5 kHz about the magic angle. Figure 1 shows the $^1H-^{13}C$ HMQC spectrum where gradients were employed to select that portion of the proton magnetization that is coupled to ^{13}C. The pulse sequence is identical to that previously described by Hurd and John.[15] The long-range proton−carbon correlation experiment (HMBC) is shown in Figure 2. Notice the excellent suppression of artifacts in both of these spectra, as seen from the noise floor in the expanded sections of the spectra. Also note the enhanced resolution of the HMBC measurement where the *J*-evolution time has been set to 50 ms and therefore broad components of the lines are suppressed.

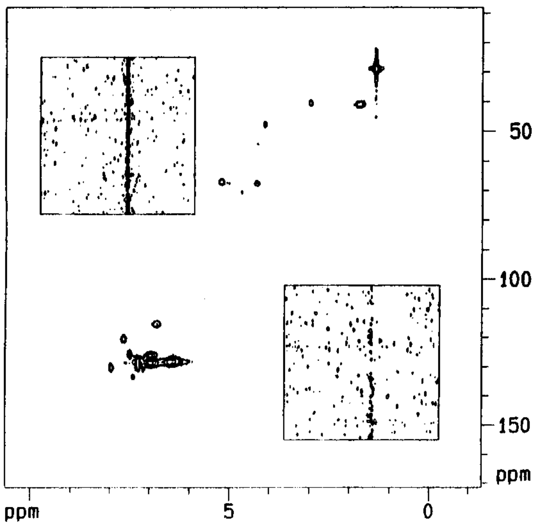

Figure 1. $^1H-^{13}C$ HMQC spectrum of an N-FMOC-N-Boc-L-Lysine derivatized Wang resin swollen with $CDCl_3$, obtained at a proton frequency of 400 MHz and at a rotor frequency of 5 kHz. Gradient pulses of 1-ms duration were used (with strengths of 10, 10, and 5 G/cm) to select magnetization only from those protons coupled to a ^{13}C. The insert in the lower right-hand corner displays the noise floor of that portion of the 2D spectrum, while the insert in the upper left-hand corner displays the noise floor from the identical area of a hr-MAS 2D spectrum acquired without the aid of gradients. Note the excellent suppression of t_1-noise shown in the noise-floor expansion in the insert.

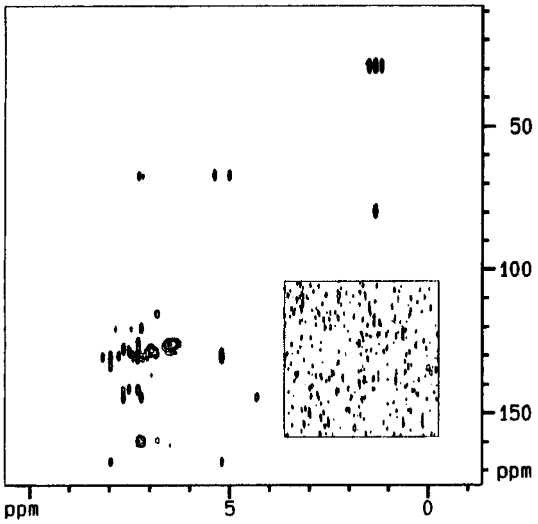

Figure 2. $^1H-^{13}C$ HMBC spectrum of the same compound and under the same experimental conditions as in Figure 1. The insert shows an expanded region of the noise floor and demonstrates the excellent artifact suppression. A *J*-evolution time of 50 ms is used to reveal long-range proton−carbon correlations. No carbon decoupling is applied during the acquisition.

These swollen resins are representative of a class of samples were hr-MAS methods are expected to yield enhanced resolution. For all of these we anticipate that gradient methods will become as common in hr-MAS as they are in high resolution liquid state measurements. In fact, one can argue that the need for gradients is more pronounced in the hr-MAS case since the probe geometry and sample spinning builds into the measurement an unavoidable modulation of the coupling of the spins to the receiver and hence pronounced artifacts.

Acknowledgment. The authors thank J. Lewandowski and M. Ziliox for technical assistance and useful discussions. This work was funded in part by the National Science Foundation (DMR-9357603) and the National Institutes of Health (ROI-GM52026, RR-00995).

Supporting Information Available: Symmetry of the gradient and a demonstration that it is indeed increasing along the axis of rotation shown by 1-D profiles of the sample volume under static and spinning conditions (3 pages). See any current masthead page for ordering and Internet access instructions.

JA962227T

---

[14] The probe used in this work is a modified Bruker widebore CP/MAS probe with a proprietary gradient set generating 5 $G \cdot cm^{-1} \cdot A^{-1}$, for which a patent application is filed. Since then a gradient set compatible with a standard bore (40 mm o.d.) probe has been developed.

[15] Hurd, R. E.; John, B. K. *J. Magn. Reson.* **1991**, *91*, 648.